Supramolecular Isomers of Metal-Organic Frameworks Derived from a Partially Flexible Ligand with Distinct Binding Motifs

Rasha G. AbdulHalim, Aleksander Shkurenko, Mohamed H. Alkordi, and Mohamed Eddaoudi*

Functional Materials Design, Discovery & Development Research Group (FMD^3), Advanced Membranes & Porous Materials Center, Division of Physical Sciences and Engineering, King Abdullah University of Science and Technology (KAUST), Thuwal 23955-6900, Kingdom of Saudi Arabia

Table of Contents

I- Materials and Methods

Powder X-ray Diffraction (PXRD) measurements were carried out at room temperature on a PANalytical X'Pert Pro diffractometer 45 kV, 40 mA for Cu$K\alpha$ (λ = 1.5418 Å), with a scan speed of 1.0° min^{-1} and a step size of 0.017° in 2θ.

Thermogravimetric analysis (TGA) was performed on a TA Instrument Hi-Res TGA Q5000IR with High Resolution TGA (Hi-Res TGA) capability. Experiments were performed under N_2 atmosphere with balance and sample purge flow rates of 10ml min^{-1} and 25 ml min^{-1}, respectively. Samples were placed on 100 µl high temperature platinum crucibles and heated in Hi-Res TGA mode with a heating rate of 5°C min^{-1} and a resolution index of 4 and a sensitivity index of 1.

Single Crystal X-ray Diffraction The single crystal X-ray diffraction data for all structures were measured on a Bruker APEX2 equipped with a Cu $K\alpha$ INCOATEC Imus micro-focus source (λ = 1.54178 Å). Indexing was performed using APEX2[1] (Difference Vectors method). Data integration and reduction were performed using SaintPlus 6.01.[2] Absorption correction was performed by multi-scan method implemented in SADABS.[3] Space groups were determined using XPREP implemented in APEX2. The structure was solved using SHELXS-97 (direct methods) and refined using SHELXL-2013[4] (full-matrix least-squares on F^2) contained in APEX2, [1, 4] WinGX v1.70.01[4-5] and OLEX2[4, 6].

II- Thermogravimetric Analysis

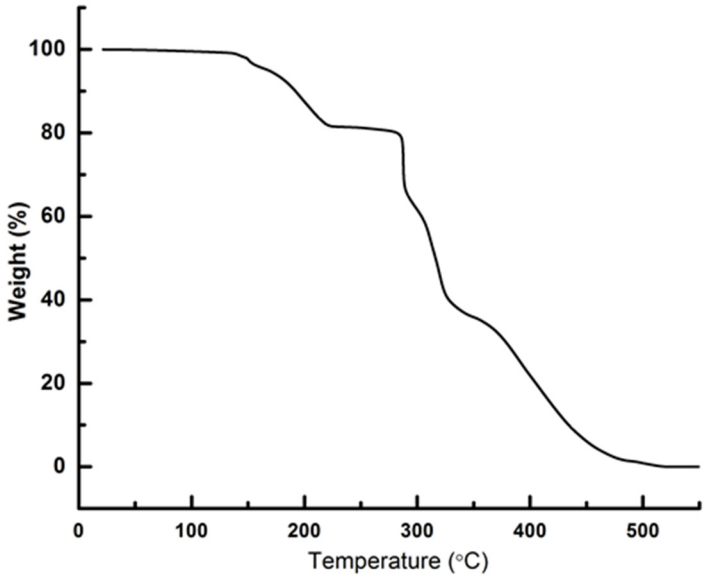

Figure S1. TGA for the as-synthesized **1**.

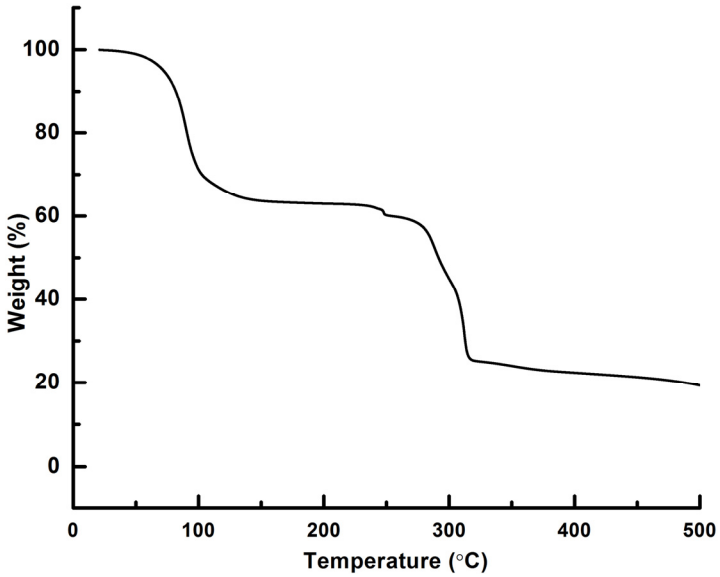

Figure S2. TGA for the as-synthesized **2**.

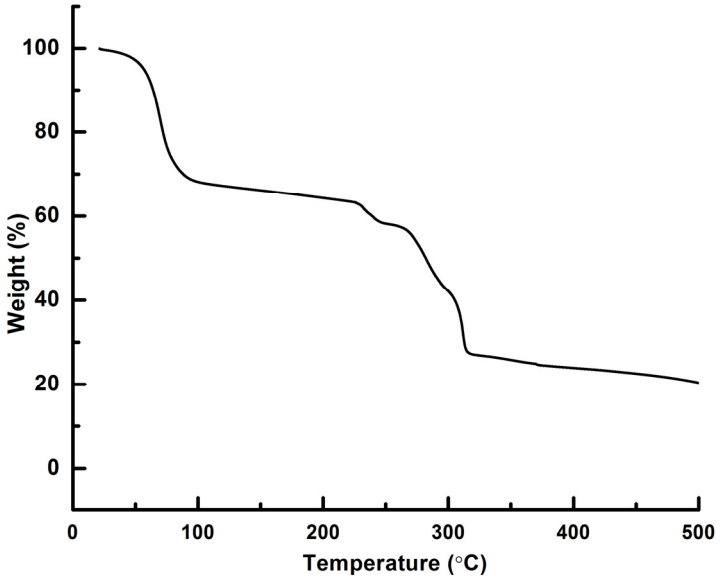

Figure S3. TGA for the as-synthesized **3**.

III- Powder X-ray Diffraction (PXRD) Patterns

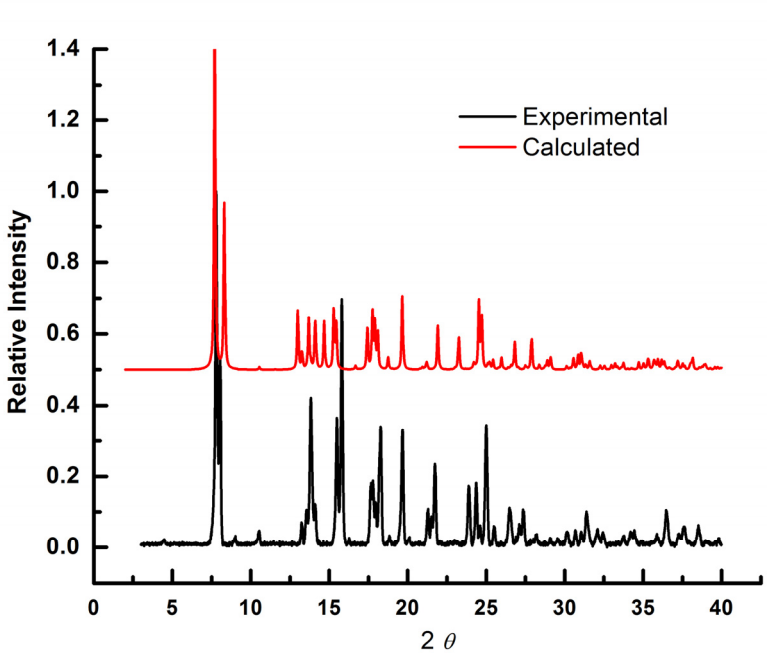

Figure S4. Comparison of the calculated and experimental PXRD patterns for **1**.

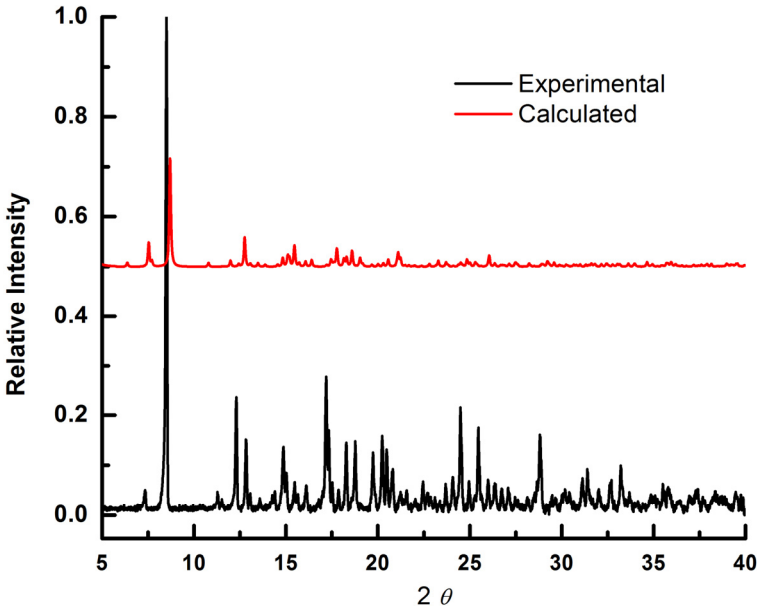

Figure S5. Comparison of the calculated and experimental PXRD patterns for **2**.

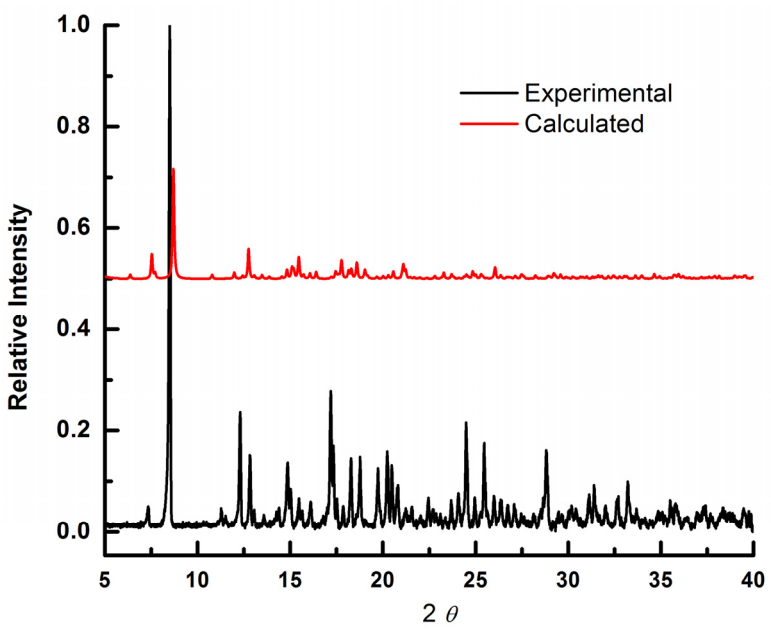

Figure S6. Comparison of the calculated and experimental PXRD patterns for **3.**

VI- Topological Analysis:

A. All points of extension considered for structures **2** and **3**

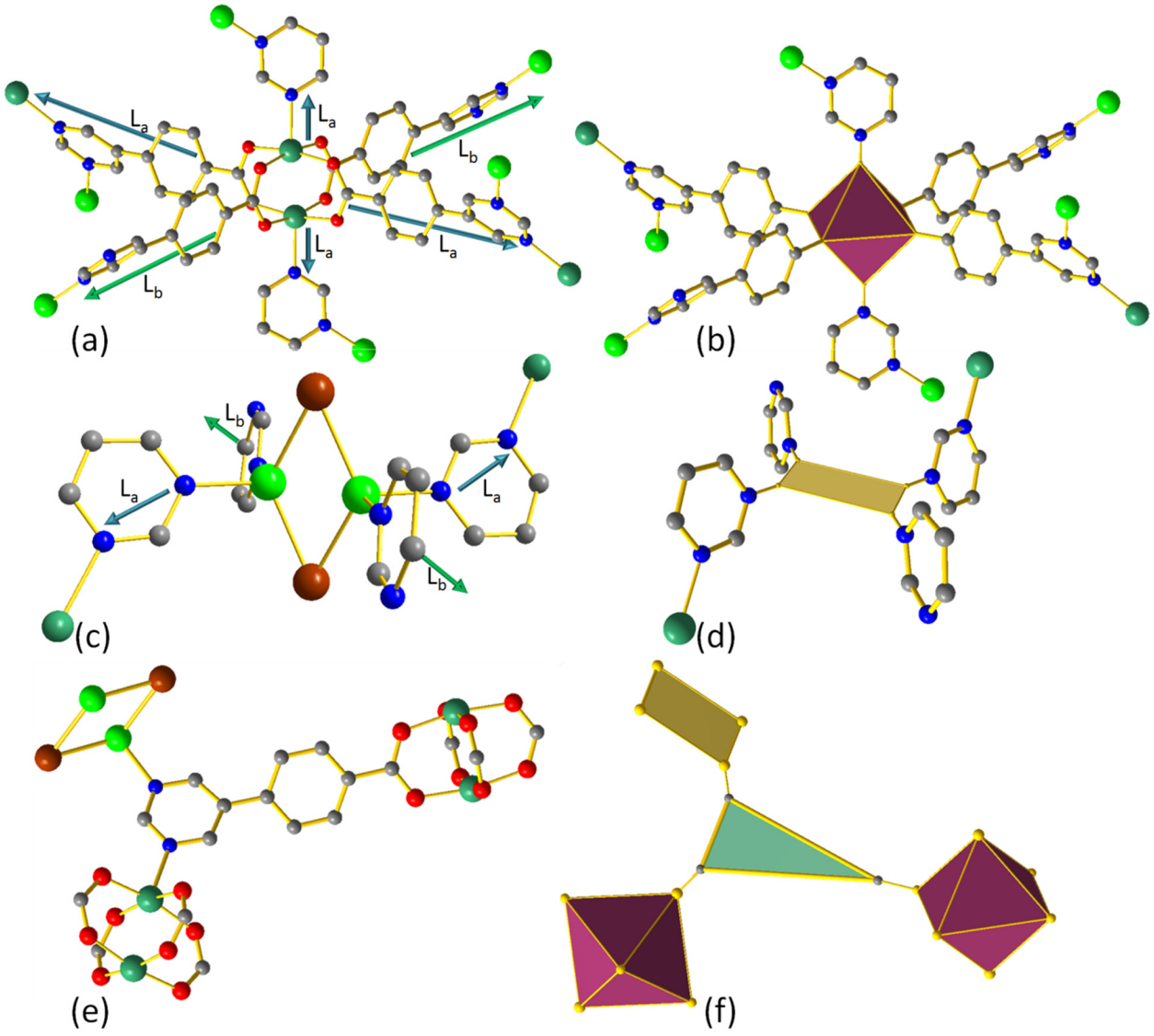

Figure S7. Schematic illustration of the MBBs and SBUs respectively: (a) and (b) representing 6-c paddlewheel, (c) and (d) representing 4-connected $[Cu_2I_2(N–)_4]$, (e) and (f) representing coordination environment of the tritopic linker L_a. Color code (Cu(I) = bright green, Cu(II) = sea green, I = brown)

B. In the absence of the rhomboid dimer [Cu_2I_2]

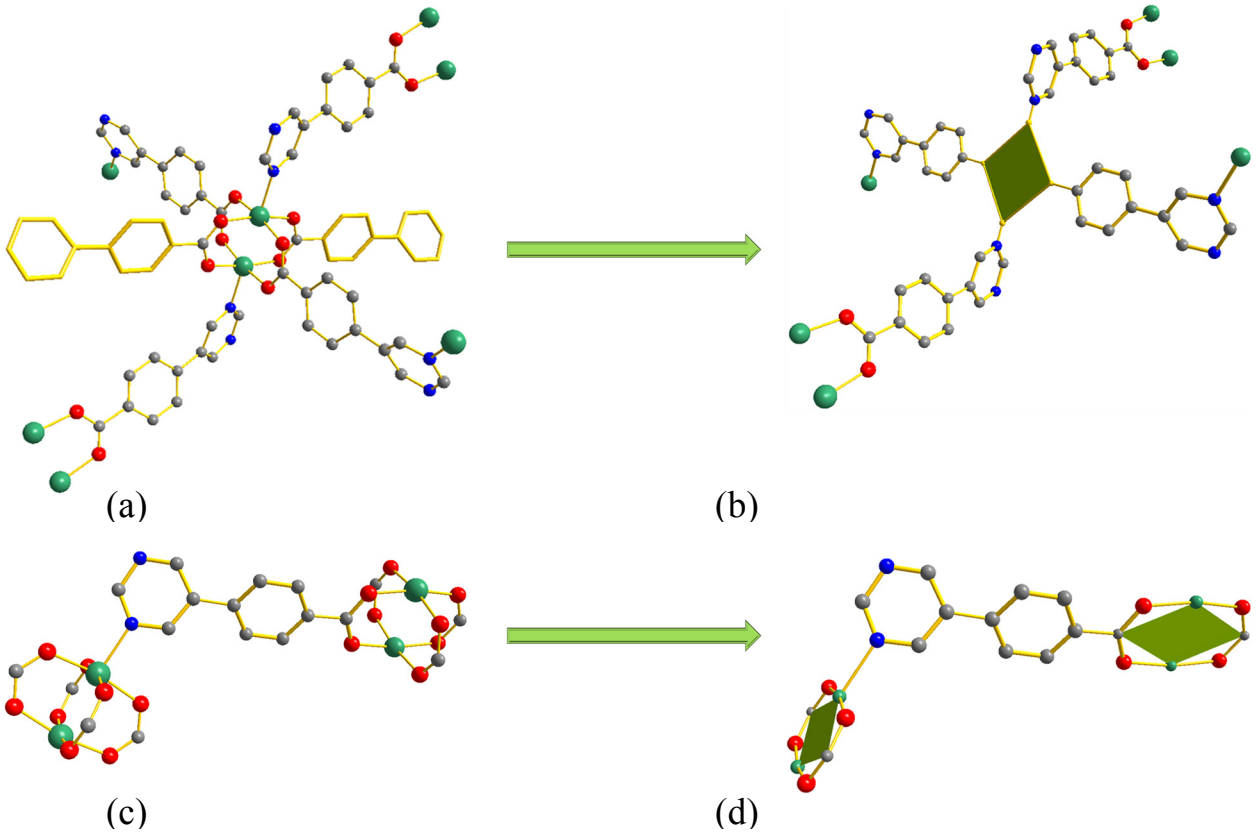

Figure S8. Schematic illustration of the MBBs and SBUs: (a) representing the coordination of the paddlewheel where L_b becomes a terminal ligand (highlighted in gold) and (b) paddle wheel is reduced to a 4-c building unit with lozenge geometry, (c) and (d) L_a becomes ditopic connecting 2 paddlewheels together. Color code (Cu(II) = sea green)

C. Associated nets underlying topologies

C.1. Structure **2**

C.1.1. All points of extension considered

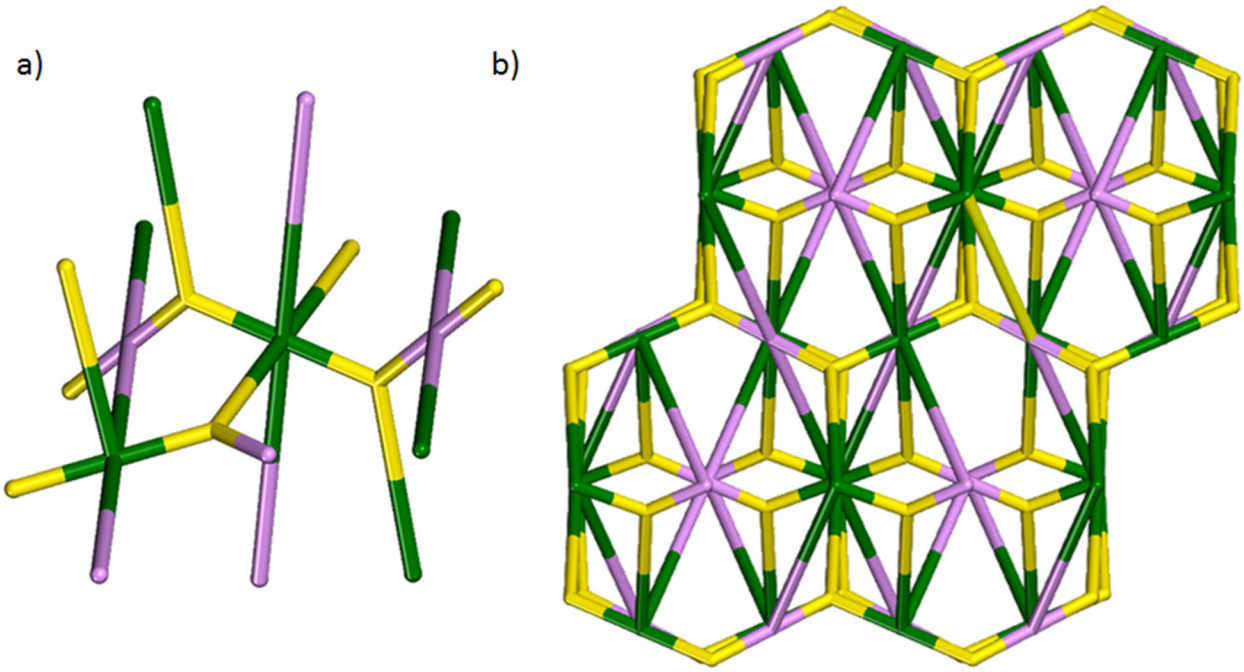

Figure S9. Topological analysis of **2**, a) each 6-c node (sea green) is connected to four 3-c nodes (yellow) and two 4-c nodes (lavender); b) illustration of (3,4,6)-connected net and its view along x-axis.

Prior to topological analysis, the structure has been simplified to its basic nodes (Figure **S8**). The two independent inorganic clusters (MBB-1 and MBB-2) are reduced to 6-connected and 4-connected nodes (**α**, **β**), respectively, while the tritopic ligand is reduced to a 3-connected node (**γ**). The topological analysis reveals that **2** exhibits a new (3,4,6)-connected topology.

Point symbol for net: $\{5^2.6\}2\ \{5^2.7^3.8\}\ \{5^4.6^2.8^2.10\}$

(3,4,6)-c net with stoichiometry (3-c) 2 (4-c) (6-c); 3-nodal net, transitivity: [3443], new topology
TD10 = 2521

Topological terms for each node:

(**α**) Point symbol: $\{5^4.6^2.7^6.8^2.10\}$
Extended point symbol:[5.5.5.5.6.6.7.7.7.7.7(3).7(3).8(2).8(2).10(6)]
Coordination sequences: 6 14 40 74 130 208 320 440 624 782

(**β**) Point symbol: $\{5^2.7^3.8\}$
Extended point symbol: [5.5.7(2).7(2).7(2).8(2)]
Coordination sequences: 4 14 36 68 124 196 306 450 586 794

(**γ**) Point symbol: $\{5^2.6\}$
Extended point symbol: [5.5.6],
Coordination sequences: 3 13 31 67 111 193 287 421 552 755

C.1.2. Omitting the $[Cu_2I_2]$ connectivity

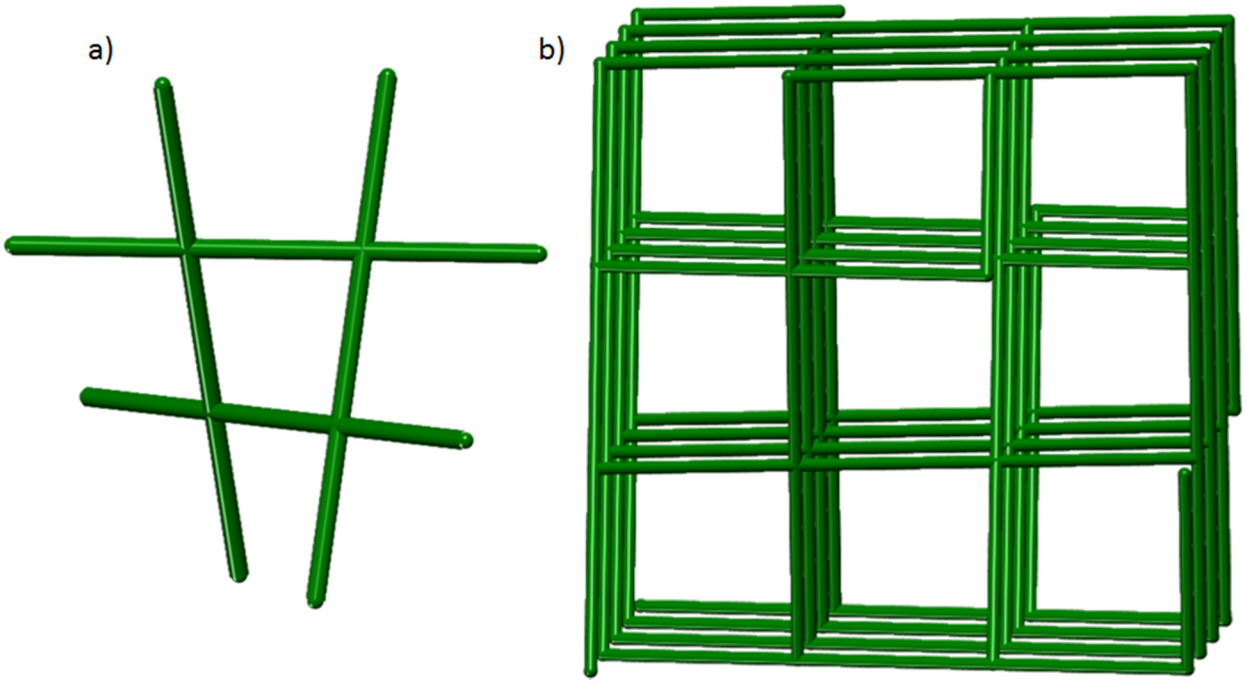

Figure S10. Topological analysis of **2** after eliminating MBB-2, (a) and (b) illustration of the unimodal net with **lvt** topology; each 4-c node (sea green) is connected to four 4-c nodes.

Prior to topological analysis, the structure has been simplified to its basic nodes (Figure **S9**). MBB-1 is reduced to a 4-connected node (**α**). The topological analysis reveals that **2** exhibits **lvt** topology.
Point symbol for net: $\{4^2.8^4\}$

4-c net uninodal net, transitivity: [1121], **lvt** topology
TD10 = 1127

Topological terms for each node:
(**α**) Point symbol: $\{4^2.8^4\}$
Extended point symbol: [4.4.8(4).8(4).8(8).8(8)]
Coordination sequences: 4 10 24 44 72 104 144 188 240 296

C.2. Structure **3**

C.2.1. All points of extension considered

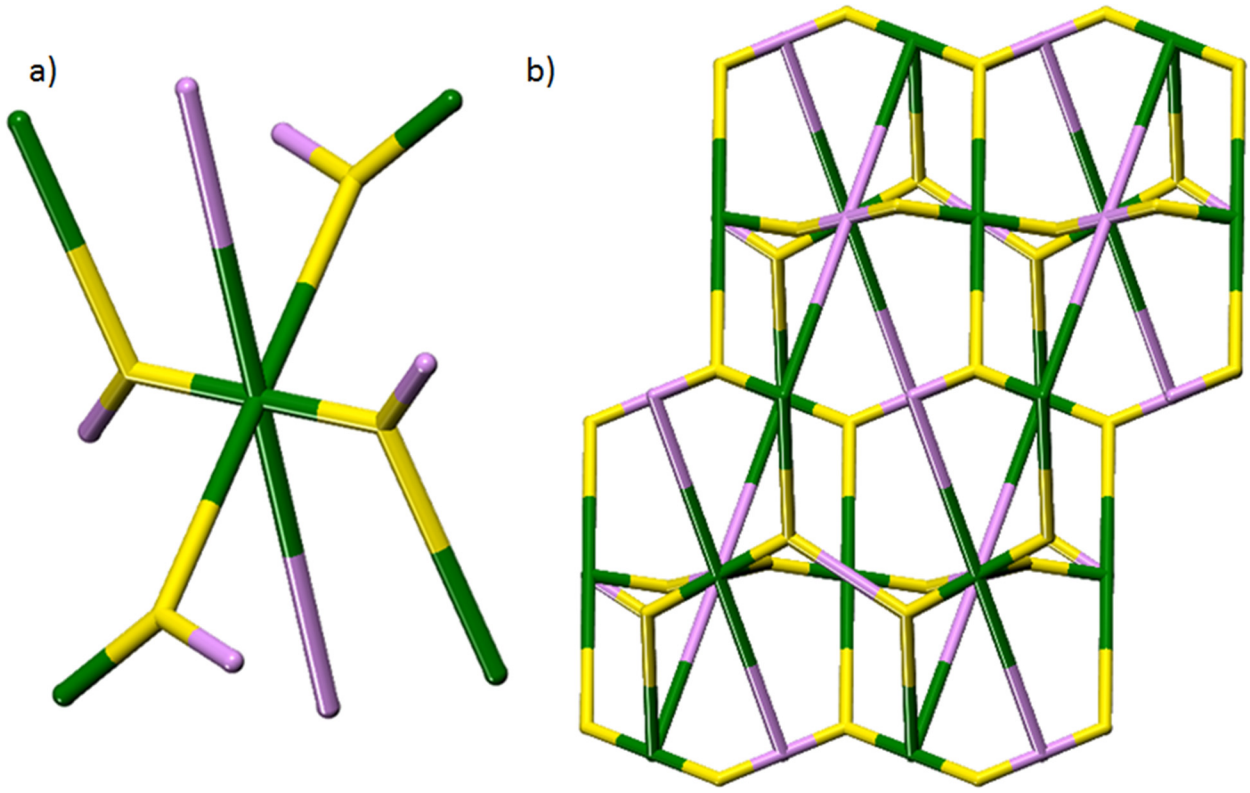

Figure S11. Topological analysis of **2**, a) each 6-c node (sea green) is connected to four 3-c nodes (yellow) and two 4-c nodes (lavender); b) illustration of (3,4,6)-connected net and its view along xz -plane.

Prior to topological analysis, the structure has been simplified to its basic nodes (Figure **S9**). The two independent inorganic clusters (MBB-1 and MBB-2) are reduced to 6-connected and 4-connected nodes (**α**, **β**), respectively, while the tritopic ligand is reduced to a 3-connected node (**γ**). The topological analysis reveals that **2** exhibits a new (3,4,6)-connected topology.

Point symbol for net: $\{5^2.6\}2\ \{5^2.7^3.8\}\ \{5^4.6^2.8^2.10\}$

(3,4,6)-c net with stoichiometry (3-c) 2 (4-c) (6-c); 3-nodal net, transitivity: [3432], new topology TD10 = 1923

Topological terms for each node:

(**α**) Point symbol: $\{5^8.6^2.8^4.9\}$
Extended point symbol:[5.5.5.5.5.5.5.5.8.8.6.6.8(2).8(4).9(2)]
Coordination sequences: 6 14 34 62 114 170 252 334 448 556

(**β**) Point symbol: $\{5^4.7.8\}$
Extended point symbol: [5.5.5.5.7(2).8(4)]
Coordination sequences: 4 14 30 58 102 166 248 330 442 544

(**γ**) Point symbol: $\{5^3\}$
Extended point symbol: [5.5.5(2)],
Coordination sequences: 3 13 26 58 98 161 232 326 417 547

C.2.2. Omitting the $[Cu_2I_2]$ connectivity

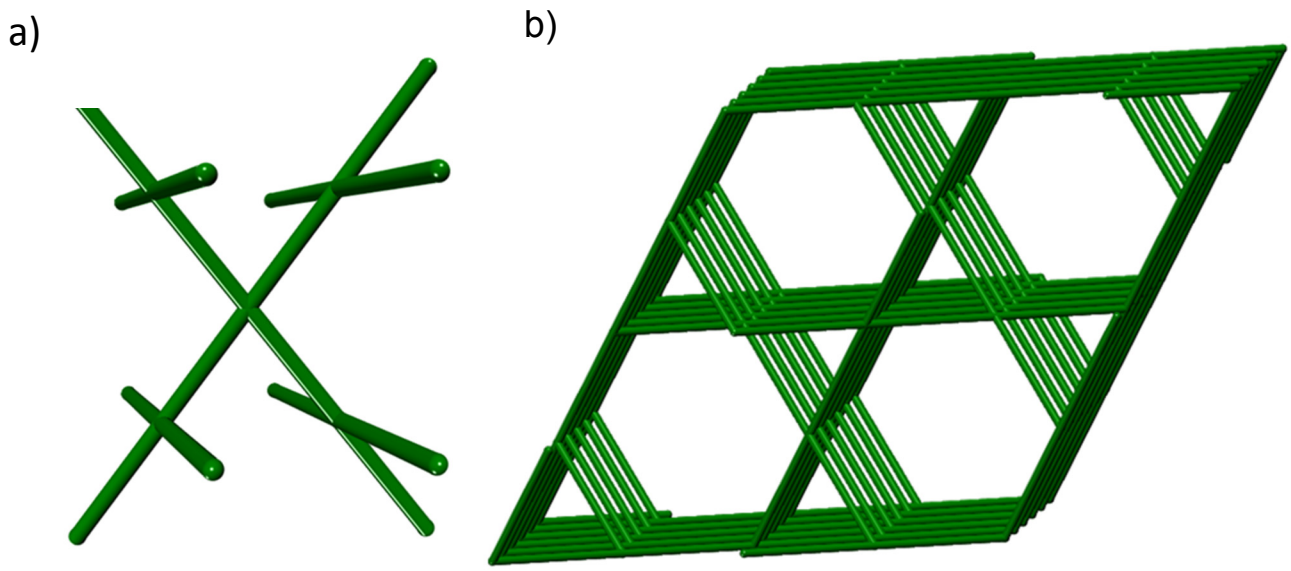

Figure S12. Topological analysis of **3** after eliminating MBB-2, (a) and (b) illustration of the unimodal net with **nbo** topology; each 4-c node (sea green) is connected to four 4-c nodes.

Prior to topological analysis, the structure has been simplified to its basic nodes (Figure **S11**). MBB-1 is reduced to a 4-connected node (**α**). The topological analysis reveals that **3** exhibits **nbo** topology.
Point symbol for net: $\{6^4.8^2\}$

4-c net uninodal net, transitivity: [1121], **nbo** topology
TD10 = 1169

Topological terms for each node:
(**α**) Point symbol: $\{6^4.8^2\}$
Extended point symbol: [6(2).6(2).6(2).6(2).8(6).8(6)]
Coordination sequences: 4 12 28 50 76 110 148 194 244 302

VII- Single Crystal X-ray Diffraction Data

Table S1. Crystal Structure Data for Compounds 1, 2 **and** 3.

	1	**2**	**3**
Empirical formula	$C_{48}H_{34}Cu_2N_{10}O_8$	$C_{66.13}H_{88.89}Cu_4I_2N_{15.38}O_{20}$	$C_{76.19}H_{90.74}Cu_4I_2N_{14.44}O_{16.83}$
Formula weight	1005.93	1927.23	1986.09
Crystal system	Monoclinic	Tetragonal	Trigonal
Space group	$P2_1/c$	$I4_1/a$	R-3
a (Å)	7.668(1)	34.018(3)	40.463(5)
b (Å)	13.624(2)	34.018(3)	40.463(5)
c (Å)	21.309(3)	15.308(1)	15.710(2)
α (°)	90	90	90
β (°)	93.599(7)	90	90
γ (°)	90	90	120
Volume (Å^3)	2221.9(6)	17715(3)	22275(6)
Z, calculated density (g cm^{-3})	2, 1.504	8, 1.445	9, 1.333
F(000)	1028	7803	9051
Temperature (K)	100.0(1)	100.0(1)	100.0(1)
Radiation type	Cu $K\alpha$	Cu $K\alpha$	Cu $K\alpha$
Absorption correction	Multi-scan	Multi-scan	Multi-scan
Absorption coefficient (mm^{-1})	1.75	7.14	6.38
Crystal size (mm)	0.03 × 0.06 × 0.09	0.09 × 0.09 × 0.18	0.09 × 0.09 × 0.24
Shape, color	Block, clear light blue	Tetragonal bipyramid, light green	Trigonal antiprism, clear light green
θ range for data collection (°)	3.9–63.7	4.1–66.9	6.2–67.5
Limiting indices	$-8 > h > 8$ $-15 > k > 14$ $-24 > l > 18$	$-40 > h > 40$ $-29 > k > 39$ $-17 > l > 18$	$-45 > h > 41$ $-44 > k > 41$ $-17 > l > 17$
Reflection collected / unique / observed with $I > 2\sigma(I)$	11167 / 3509 / 3280	90211 / 7746 / 7326	25823 / 7515 / 7278
R_{int}	0.025	0.068	0.031
Refinement method	Full-matrix least-squares on F^2	Full-matrix least-squares on F^2	Full-matrix least-squares on F^2
Data / restraints / parameters	3509 / 0 / 308	88061 / 106 / 511	7515 / 132 / 587
Final R indices [$I > 2\sigma(I)$]	$R_1 = 0.031$, $wR_2 = 0.085$	$R_1 = 0.063$, $wR_2 = 0.152$	$R_1 = 0.042$, $wR_2 = 0.108$
Final R indices (all data)	$R_1 = 0.033$, $wR_2 = 0.086$	$R_1 = 0.072$, $wR_2 = 0.155$	$R_1 = 0.043$, $wR_2 = 0.109$
Weighting scheme	$[\sigma^2(F_o^2) + (0.0491P)^2 + 1.8134P]^{-1}$	$[\sigma^2(F_o^2) + (0.0535P)^2 + 332.3661P]^{-1}$	$[\sigma^2(F_o^2) + (0.0522P)^2 + 192.9264P]^{-1}$
Goodness-of-fit	1.05	1.05	1.02
Largest diff. peak/hole / e Å^{-3}	0.46/-0.39	1.18/-1.13	1.28 / -1.26

VIII- References

1. Inc, B. A. *APEX2 (Version 2013.6-2)*, Bruker AXS Inc: Madison, Wisconsin, USA, 2013.
2. Bruker *SAINT-V8.32A*, Bruker AXS. Inc: Madison, Wisconsin, USA, 2013.
3. Sheldrick, G. M. *SADABS*, University of Gottingen, Germany, 1996.
4. Sheldrick, G. M. *Acta Crystallogr. Sect. A* **2008,** *64*, 112-122.
5. (a) Farrugia, L. *J. Appl. Crystallogr.* **1999,** *32* (4), 837-838; (b) Sheldrick, G. M. *SHELXL-97*, 1997; (c) Sheldrick, G. M. *Acta Crystallogr. Sect. A* **1990,** *46*, 467-473.
6. Dolomanov, O. V.; Bourhis, L. J.; Gildea, R. J.; Howard, J. A. K.; Puschmann, H. *J. Appl. Crystallogr.* **2009,** *42*, 339-341.